Cherry stones-based activated carbons as potential adsorbents for CO_2/CH_4 separation: Effect of the activation parameters

N. Álvarez-Gutiérrez, M.V. Gil, F. Rubiera, C. Pevida*

Instituto Nacional del Carbón, INCAR-CSIC, Apartado 73, 33080 Oviedo, Spain

Abstract

A low-cost biomass, cherry stones (CS), was used as carbon precursor to synthesize two activated carbons to be used for CO_2/CH_4 separation. Single-step activation with two activating agents, carbon dioxide and steam, was used. The activation conditions that maximize the CO_2 adsorption capacity by the adsorbents at 25 ºC and atmospheric pressure were determined by response surface methodology (RSM). The optimum values were 885 ºC and 12% of solid yield when activating with carbon dioxide, but 850 ºC and 15.3% of solid yield when activating with steam. Heating rate did not show a significant effect on the CO_2 uptake. CO_2 adsorption capacity values up to 11.45 and 10.56 wt.% were achieved under such conditions using carbon dioxide and steam as activating agents, respectively. Carbon dioxide activation promoted the development of microporosity, whereas both micropores and mesopores were developed during steam activation. The CO_2/CH_4 separation performance at 3 bar of the optimum adsorbents indicated that both cherry stones-based activated carbons could have great potential as CO_2 adsorbents for CO_2/CH_4 separation. The adsorbent activated with carbon dioxide, CS-CO_2, showed a slightly higher adsorption capacity, but the steam activated sample, CS-H_2O, had an enhanced selectivity to separate CO_2 from CO_2/CH_4 binary mixtures.

* Corresponding author. Tel.: +34 985 119 090; Fax: +34 985 297 662

E-mail address: cpevida@incar.csic.es (C. Pevida)

Keywords: Activated carbon; Cherry stones; CO_2/CH_4 separation; CO_2 uptake; Response surface methodology

1 INTRODUCTION

Biogas is produced from the decomposition of organic wastes, and is rich in CH_4 (35-75 vol.%). Its release into the atmosphere largely contributes to greenhouse gas concentration. However, the energetic content of the biogas is high (higher heating value of 15-30 MJ Nm^{-3}) and its exploitation involves significant revenues or avoided costs.[1]

CO_2 is present in the biogas in large quantities (almost balanced to the percentage of CH_4), and as it is an inert gas in terms of combustion, it decreases the energetic content of the biogas. The main technology used for enriching biogas in CH_4 by means of CO_2 separation is pressure swing adsorption (PSA) on zeolites, due to their high selectivity towards CO_2. Nevertheless, activated carbons (ACs) can be promising materials for CO_2/CH_4 separation due to their high adsorption capacity at atmospheric pressure, hydrophobic character, significant lower cost than zeolites, high surface area and amenability to pore structure modification and surface functionalization.[2] Moreover, a lower amount of energy is needed to regenerate activated carbons compared to zeolites. Some of the requirements that need to fulfil the ACs in order to be competitive materials for CO_2/CH_4 separation purposes are availability, high stability, ease of regeneration and low cost, as well as high CO_2 selectivity and adsorption capacity. Carbon adsorbents can be obtained at low cost if a renewable, relatively abundant and globally available source, such as biomass, is used as precursor material.

The production of carbon adsorbents from biomass precursors can involve physical or chemical activation to develop the porosity.[3] The adsorption capacity of an

AC is mainly dependent on its pore structure. In the present work, physical activation was selected due to its lower energy consumption and processing time, as well as it has a lower environmental impact when using CO_2, H_2O or air as activating agent. Physical activation is generally carried out in a two-step procedure: carbonization and activation. Single-step activation has been less explored, although good adsorption characteristics for removal of NO_2 from air or pollutants from water have been reported in literature after biomass activation by a single-step procedure using CO_2 or steam as activating agents.[4-7] Single-step activation was therefore selected in the present work for preparing cherry stones-based activated carbons.

Every carbon precursor requires specific activation conditions, and so an increase in the activation degree could only be justified if a significant improvement in the adsorption capacity of the adsorbent was observed. Therefore, CO_2 adsorption on the activated carbons prepared in the present work was optimized in relation to temperature, heating rate and solid yield during the single-step activation by means of response surface methodology (RSM). RSM is a statistical technique which has lately been applied in research related with CO_2 capture to evaluate the effects of several factors and determine the optimum conditions for the studied process.[8,9] It uses the design of experiments and the multiple regression analysis to model the relationship between several independent variables and a response variable.[10]

The commercial synthesis of activated carbons is currently demanding cheap, easily accessible and widely available precursors. An agricultural by-product, such as cherry stones (CS), is abundant in Spain, especially in the regions of Extremadura and Aragón, from the industrial production of Kirsch (cherry brandy) and jam. The cherry stones could be recycled by means of the production of activated carbons, since they

71 constitute a source of renewable carbon with a low cost. In addition, they are suitable
72 for preparing microporous activated carbons due to their low ash content. To the best of
73 our knowledge, few studies have been published on the preparation of activated carbons
74 from cherry stones, which were synthesized by conventional two-step activation and
75 they were characterized and evaluated for adsorbing gases such as NO_2 or H_2S and
76 liquid impurities.[11-14] However, studies on one-step CO_2 or steam activation of cherry
77 stones have not been reported in literature. Therefore, in the present work two
78 microporous activated carbons were for the first time prepared from cherry stones by
79 single-step activation with carbon dioxide and steam for application in CO_2/CH_4
80 separation. CO_2 adsorption on these adsorbents was optimized in relation to the
81 activation conditions (temperature, heating rate and solid yield) by means of RSM.
82 Afterwards, two activated carbons were produced on a larger scale using the resulting
83 optimum activation conditions and were texturally characterized. The performance to
84 separate CO_2 from CO_2/CH_4 binary mixtures, representative of biogas streams, was
85 evaluated.

86 **2 EXPERIMENTAL**

87 **2.1 Single-step activation with CO_2 or steam**

88 A low-cost biomass, cherry stones (CS), was used as starting material. Cherry
89 stones were ground and sieved, and samples with a particle size between 1 and 3 mm
90 were selected. The proximate and ultimate analyses of the raw material are collected in
91 Table 1. The single-step activation with carbon dioxide or steam was carried out in a
92 Setaram TAG24 thermobalance, methodology previously validated in our laboratory.[15]
93 Accordingly, in order to choose the activation temperature range, non-isothermal mass
94 loss profiles of raw CS under carbon dioxide and steam up to 1000 ºC were conducted

95 (data not shown). The temperature of commencement of mass loss, after the loss of
96 moisture and volatile matter, was taken as the minimum activation temperature. Thus, a
97 range of activation temperature of 750-950 ºC was selected for the subsequent statistical
98 study with both activating agents.

99 Given that single-step activation does not include a preliminary carbonization
100 step, the term "solid yield" instead of "burn-off degree" was preferred in the present
101 work. The solid yield was calculated by dividing the mass of the resulting activated
102 carbon by the initial mass of the dried precursor. Samples of approximately 40 mg were
103 used. In the case of the carbon dioxide activated adsorbents, the cherry stones samples
104 were physically activated in a 100 mL min^{-1} stream of CO_2, whereas for the steam
105 activated carbons, the activation was carried out under a 100 mL min^{-1} stream
106 containing 35 vol.% of H_2O (balance N_2). Prior to activation the samples were dried at
107 100 ºC under an inert atmosphere of N_2. The duration of the activation process was
108 dependent on the solid yield targeted in each experiment.

109 The preparation of the two optimum activated carbons on a larger scale
110 following the experimental conditions determined from the above study was carried out
111 in a vertical furnace from Carbolite. Samples of approximately 10 g were activated
112 under the same conditions used in the thermobalance.

113 **2.2 Response surface methodology**

114 Response surface methodology was used to optimize the activation variables
115 that maximize the CO_2 adsorption capacity at 25 ºC and atmospheric pressure of each
116 cherry stones-based activated carbon. Three independent variables were evaluated:
117 activation temperature (*T*) between 750 and 950 ºC, heating rate (*HR*) between 10 and
118 20 ºC $min^{-1}$and solid yield after activation (*Y*) between 7 and 17% for CS activated with

carbon dioxide and between 7 and 22% for CS activated with steam. The response or dependent variable, which is measured during the experiments, was the CO_2 uptake.

The experimental design selected in this study was the central composite design (CCD), which consists of the following parts: (1) a full factorial design; (2) a star design in which experimental points are at a certain distance, α, from its centre and (3) a replicated central point. The α-value depends on the number of variables, k, and can be calculated by $\alpha=2^{k/4}$; for three variables, it is 1.682. The CCD design involved 20 experiments, including eight factorial points (2^3 full factorial design), six axial points and six replicates of the centre of the design. The experiments were conducted in a random order. Prior to the application of RSM, the independent variables were coded in dimensionless values so that variables with different units or of different orders of magnitude could be compared. The coded (in parentheses) and the decoded values of the independent variables (T, HR and Y), together with the experimental results obtained for the response variable (CO_2 uptake) are shown in Table 2 for the carbon dioxide activated-CS and steam activated-CS adsorbents, respectively.

The experimental data collected from CCD for the three independent variables, x_1 (T), x_2 (HR) and x_3 (Y), were mathematical-statistically fitted to the following second-order polynomial model:

$$y = \beta_0 + \beta_1 x_1 + \beta_2 x_2 + \beta_3 x_3 + \beta_{11} x_1^2 + \beta_{22} x_2^2 + \beta_{33} x_3^2 + \beta_{12} x_1 x_2 + \beta_{13} x_1 x_3 + \beta_{23} x_2 x_3 + \beta_{123} x_1 x_2 x_3 + \varepsilon \quad (1)$$

where y is the response variable; β_0 is the constant term; β_1, β_2 and β_3 are the coefficients of the linear parameters; β_{11}, β_{22} and β_{33} are the coefficients of the quadratic parameters; β_{12}, β_{13}, β_{23} and β_{123} are the coefficients of the interaction parameters and ε is the residual associated with the experiments. The experimental data were fitted to Eq. (1)

143 by multiple regression analysis (least squares) and the β coefficients that generate the
144 lowest possible residual were determined. The fitness of the quadratic model to the
145 experimental data was evaluated by analysis of variance (ANOVA) and lack-of-fit tests.
146 A model was considered to fit the experimental data well when it showed a significant
147 regression (p-value<0.05 to a confident level of 95%) and a non-significant lack of fit
148 (p-value>0.05 to a confident level of 95%). The accuracy of the fitted polynomial model
149 was expressed by the coefficient of determination R^2 and by Adj-R^2, which penalizes the
150 statistic R^2 as extra variables are included in the model. The absolute average deviation
151 (AAD) was also calculated in order to check the accuracy of the model. ADD describes
152 the deviations between the experimental and calculated values. It must be as small as
153 possible and is calculated as follows:[16]

154 $$\text{AAD } (\%) = 100\left[\sum_{i=1}^{n}\left(\frac{\left|y_{i,\text{exp}} - y_{i,\text{calc}}\right|}{y_{i,\text{exp}}}\right)\right]\Big/ n \qquad (2)$$

155 where $y_{i,\text{exp}}$ and $y_{i,\text{calc}}$ are the experimental and calculated responses, respectively, and n
156 is the number of experiments. The statistical analyses were carried out using SPSS
157 Statistics 21.0 software.

158 To visualize the combined effects of two factors on the response, the three-
159 dimensional plot of the model, i.e., response surface plot, was obtained. The two-
160 dimensional display of the surface plot generates the contour plot, where the lines of
161 constant response are drawn on the plane of the two independent variables. Response
162 surface and contour plots were generated using the SigmaPlot 10.0 software. Then, the
163 optimum values for each independent variable that would produce the best response in
164 the experimental region under study were determined.

165 **2.3 CO_2 uptake**

166 The CO_2 capture capacity of the adsorbents was evaluated in a Setaram TAG24
167 thermogravimetric analyser at 25 ºC and atmospheric pressure. Prior to the adsorption
168 measurements, the samples (approximately 40 mg) were dried in situ. Afterward, a CO_2
169 adsorption test was conducted under a CO_2 flow rate of 100 mL min^{-1} at 25 ºC up to
170 constant mass. The maximum CO_2 uptake at atmospheric pressure and 25 ºC was
171 evaluated from the increase in mass experienced by the sample and it was expressed in
172 terms of mass of CO_2 per mass of dry adsorbent.

173 **2.4 Textural characterization of the optimum activated carbons**

174 The porosity in the optimum cherry stones-based ACs was determined by means
175 of physical adsorption of N_2 at -196 ºC and CO_2 at 0 ºC in volumetric devices from
176 Micromeritics. This allows the assessment of the porosity in the samples from the
177 mesopores (sizes between 2 and 50 nm) down to the narrowest micropores (sizes less
178 than 0.7 nm). The usefulness of both adsorptives to characterize the porosity of carbon
179 materials has been previously reported.[17] Moreover, considering the wide range of
180 micropore size distributions that could be achieved during physical activation of a
181 carbonaceous precursor, the combination of the two adsorptives is critical to tailor the
182 characteristics of the AC for a specific application.

183 The apparent surface area was calculated from the N_2 isotherms using the
184 Brunauer-Emmett-Teller equation (S_{BET})[18] in the relative pressure range 0.01-0.1,
185 whereas the total pore volume (V_p) was estimated from the amount of nitrogen adsorbed
186 at a relative pressure of 0.99. It is known that the CO_2 capture performance of carbon
187 materials mainly involves the microporosity in the samples, so the Dubinin-
188 Radushkevich (D-R) equation[19] was used to estimate the micropore volume, W_0, and
189 the characteristic energy, E_0, as realized by the corresponding molecular probe, N_2 or

190 CO_2. The average micropore width, L_0, of the locally slit-shaped micropores is related
191 to the characteristic energy by means of the Stoeckli-Ballerini relation[20], as follows:
192 L_0 (nm) = 10.8/(E_0 (kJ mol^{-1}) - 11.4) (3)
193 In addition, the micropore volume corresponds to $W_0 = (S_{mic}/2)\ L_0$, assuming a
194 slit-shaped geometry and, consequently, the surface area of the micropore walls can be
195 estimated by the geometrical relation:[21]
196 S_{mic} ($m^2\ g^{-1}$) = 2000 W_0 ($cm^3\ g^{-1}$)/L_0 (nm) (4)
197 The micropore size distributions in the range of 0.3-1 nm were estimated by
198 means of the Non Local Density Functional Theory (NLDFT) on a slit pore carbon
199 model applied to the CO_2 adsorption isotherms.[22]
200 **2.5 Adsorption and separation of CO_2/CH_4 tests on the optimum activated carbons**
201 The adsorption isotherms of pure CO_2 and CH_4 of the cherry stones-based ACs
202 prepared under the optimum activation conditions were measured up to 10 bar at 30 ºC
203 in a high pressure magnetic suspension balance (Rubotherm-VTI). Details on the set-up
204 and the experimental procedure can be found elsewhere.[23] The absolute amounts of CO_2
205 and CH_4 adsorbed over the pressure range tested were estimated following the
206 procedure described in García *et al.*[24]
207 The experimental CO_2 and CH_4 adsorption isotherms of the cherry stones-based
208 ACs were fitted to the Sips model according to the following expression:
209 $$q = q_s \frac{(bP)^{1/n}}{1+(bP)^{1/n}} \quad (5)$$
210 where q represents the concentration of the adsorbed specie and q_s the saturation
211 capacity, P the pressure of the adsorptive and b the affinity constant. The parameter n
212 shows the heterogeneity of the system and its value is usually greater than unity;

therefore, the larger the value of n, the more heterogeneous is the system. The fitting of the experimental data to the Sips model was conducted by means of the *Solver Excel* tool assuming q_s and n to be equal for both CO_2 and CH_4 and departing from values of q_s and n of 1 and b_{CO2} and b_{CH4} of 0. The goodness of the fit was evaluated on the basis of the minimum squared relative error *(SRE)* as given by the following expression:

$$SRE(\%) = \sqrt{\frac{\sum_i \left[\left(q_{\exp,i} - q_{\mathrm{mod},i}\right)/q_{\exp,i}\right]^2}{N-1}} \times 100 \qquad (6)$$

where $q_{\exp,i}$ and $q_{\mathrm{mod},i}$ are the experimental and Sips-predicted adsorbed amounts, respectively, and N is the total number of experimental data points.

Using the fitted parameters from the pure component adsorption data, the adsorption data from a binary mixture of CO_2 and CH_4 may be predicted by an extended Sips model, similarly to the extended Langmuir equation for multicomponent adsorption. Rudziński *et al.*[25] stated that the application of the Ideal Adsorbed Solution Theory (IAST) with the concept of hypothetical pure-component pressure for normal activated carbons results in the following equation:

$$q_i = \frac{q_s b_i y_i P \left(\sum_{k=1}^{N} b_k y_k P\right)^{(1/n)-1}}{1 + \left(\sum_{k=1}^{N} b_k y_k P\right)^{1/n}} \qquad (7)$$

Eq. (8) stands for the Sips multicomponent model where i represents the species for which the isotherm q_i is being evaluated, y is the mole fraction of the corresponding component (denoted by subscript i or k) in the gas phase, and N is the total number of components in the gas mixture.

3 RESULTS AND DISCUSSION

3.1 Effect of the activation parameters on CO_2 adsorption capacity of activated carbons: Response surface methodology

Table 3 shows the results of fitting Eq. (1) to the experimental data of both activated carbons, carbon dioxide activated-CS and steam activated-CS, by multiple regression analysis and those obtained from evaluating the fitness of the model by means of ANOVA, together with the R^2, Adj-R^2 and AAD values. The coefficient values of the polynomial models presented in Table 3 are coded coefficients. Thus comparison of these values for a given material gives information of the relative influence of each independent variable on the response. The ANOVA tests showed that the models for the CO_2 capture capacity obtained were statistically significant to a 95% level of confidence (p-value<0.05), whereas their lack of fit was found to be statistically non-significant to a 95% confidence level (p-value>0.05). Table 3 also shows which terms of the models are statistically significant to a 95% confidence level *(p*-value<0.05); those that were not statistically significant (p-value>0.05) were later eliminated in the final models. The variable *HR* does not present a statistically significant effect on the CO_2 capture capacity for any studied material, CO_2 or steam activated. Lua and Guo[4] prepared activated carbons from oil palm stones by one-step CO_2 activation and they also found that the heating rate had no significant effect on the porosity development of the adsorbents. On the contrary, Yang *et al.*[5] observed very slight increases in the texture development when heating rate was raised from 5 to 10 ºC min^{-1}.

No interaction effects between *T*, *HR* and *Y* were detected in the experimental region under study, since the *T·HR*, *T·Y*, *HR·Y* and *T·HR·Y* interaction terms in the models proved to be statistically non-significant to a 95% confidence level *(p*-

257 value>0.05), as it is shown in Table 3. Once the non-significant terms were eliminated
258 from the models, the coded coefficient values were decoded in order to obtain the
259 polynomial equations that address the response variables as a function of the actual
260 independent variables. The models obtained for both activated carbons were the
261 following:

262 CO_2 uptake $_{\text{carbon dioxide activated-CS}}$ (wt.%) = –60.71300 + 0.15307 T + 0.73377 Y

263 $$- 0.00009\ T^2 - 0.03057\ Y^2 \quad (9)$$

264 CO_2 uptake $_{\text{steam activated-CS}}$ (wt.%) = –23.07866 + 0.06211 T + 0.94793 Y

265 $$- 0.00004\ T^2 - 0.03103\ Y^2 \quad (10)$$

266 Fig. 1 represents the response surface and contour plots for the CO_2 capture
267 capacity as a function of the significant independent variables, i.e., activation
268 temperature and solid yield, for carbon dioxide activated-CS (Fig. 1a) and steam
269 activated-CS (Fig. 1b). For both activated carbons, the curve-shaped response surface
270 and contour plot isolines clearly indicate that a maximum response is achieved in the
271 temperature and solid yield ranges studied, i.e., within the experimental region
272 considered.

273 For the carbon dioxide activated-CS adsorbent (Fig. 1a), the highest CO_2 capture
274 capacity (11.45 wt.%) was achieved at an activation temperature of 885 ºC and a solid
275 yield of 12%. This means that as the activation temperature increases from 750 ºC, a
276 marked increase in the CO_2 capture capacity is observed up to a maximum value.
277 However, when the activation temperature increases above 885 ºC, a slight decrease is
278 observed in the CO_2 uptake up to 950 ºC. An optimum solid yield can be also identified,
279 although this parameter has a lower influence on the response. This is indicated by the
280 lower coded coefficient for the Y term compared to that for the T term in Table 3.

281 Therefore, temperature is the most influential activation parameter on the CO_2 uptake of
282 the carbon dioxide activated-CS adsorbent. This fact suggests that an increase in the
283 activation temperature (up to 885 ºC) is more efficient in raising the CO_2 capture
284 capacity of the synthesized adsorbent than a similar decrease in coded units in the solid
285 yield between 17 and 12%.

286 For the steam activated-CS activated carbon (Fig. 1b) the highest CO_2 capture
287 capacity (10.56 wt.%) was however attained at an activation temperature of 850 ºC and
288 a solid yield of 15.3%. Even though an optimum activation temperature can be observed
289 for steam activated-CS, this parameter shows little influence on the response. Thus, the
290 CO_2 capture capacity is only slightly affected by temperature at a given solid yield. In
291 this case, as the solid yield decreases from 22%, a strong increase in the CO_2 uptake is
292 observed up to a maximum value. Nevertheless, when the solid yield decreases below
293 15.3%, the CO_2 adsorption capacity rapidly drops. The solid yield is therefore the most
294 influential activation parameter on the CO_2 capture capacity for the steam activated-CS
295 adsorbent. This can also be inferred from the higher coded coefficient of the *Y* term
296 compared to that of the *T* term in Table 3. From all these results, it is also confirmed
297 that, in the experimental region studied, the activation parameters do not similarly
298 influence the capture capacity of both ACs.

299 Higher solid yields are the result of lower activation degrees. Thus, the existence
300 of a maximum in the CO_2 capture capacity indicates that at low temperatures and
301 activation degrees (high solid yields) the extent of the activation is too weak and hence
302 the microporosity development in the materials is poor. However, when temperature
303 and activation degree are increased (lower solid yields), the CO_2 capture capacity rises
304 up to the maximum value. Then, a further increase in temperature and activation reduce

305 the microporosity in the samples due to the collapse of adjacent pore walls; this results
306 in lower CO_2 uptakes.

307 The highest CO_2 uptake at atmospheric pressure and 25 ºC corresponded to the
308 carbon dioxide activated-CS adsorbent, which reached 11.45 wt.%, but a relatively high
309 CO_2 uptake value (10.56 wt.%) was also attained by steam activated-CS. This could
310 indicate that a higher micropore volume might be expected by means of CO_2 activation
311 compared to steam, since it has been shown that adsorbents with high volumes of
312 micropores in the narrow micropore size domain are required to maximize CO_2
313 adsorption capacity at low pressures and room temperature.[26,27]

314 When steam is used as activating agent, the maximum CO_2 uptake is achieved at
315 a temperature of 850 ºC, indicating that the optimum textural development for this
316 application may be reached; higher temperature values would lead to extensive
317 gasification, ruining the porosity created and hence reducing the adsorption capacity.
318 However, when a less reactive gas such as carbon dioxide is used as activating agent,
319 activation proceeds slower and higher temperatures, 885 ºC in the present study, are
320 needed to reach the optimum textural development and consequently the maximum CO_2
321 uptake. Moreover, a longer activation time (lower solid yield) is also needed to reach
322 the optimum development of the carbon porosity when activating with carbon dioxide.
323 In single-step activation of biomass residues under oxygen atmospheres, it has been
324 found that the combination of a less reactive activating agent (i.e., air with a reduced
325 oxygen content) together with a higher activation temperature further develops the
326 narrowest pores, those with greater adsorption potential and therefore being more
327 effective for adsorbing CO_2 at ambient conditions.[28] On the other hand, Gergova and
328 Eser[7] highlighted that the evolution of porosity is much more difficult to control during

329 activation with steam than that with CO_2 due to the higher reactivity of the solid carbons
330 under steam conditions compared to CO_2. Therefore, the lower reactivity of the CS
331 precursor under a carbon dioxide atmosphere compared to steam has probably
332 influenced the higher CO_2 uptake found when the activation was carried out with carbon
333 dioxide. Even at lower temperatures, the reaction rates of the carbon material with
334 steam might be higher than with carbon dioxide, which would accelerate the
335 development of the porosity.

336 According to the results from the RSM study, the temperature, heating rate and
337 solid yield values selected for the activation in the vertical tube furnace were as follows:
338 885 ºC, heating rate of 15 ºC min^{-1} and 12% of solid yield for the optimum CS activated
339 with carbon dioxide; and 850 ºC, heating rate of 15 ºC min^{-1} and 15.3% of solid yield
340 for the CS activated with steam. These two optimum samples will be referred to as
341 CS-CO_2 and CS-H_2O, respectively, hereafter.

342 **3.2 Textural characterization of the optimum activated carbons**

343 In Fig. 2, the N_2 and CO_2 adsorption isotherms at -196 and 0 °C, respectively,
344 are plotted. Table 4 summarizes the textural parameters calculated from these isotherms.
345 Both ACs are mainly microporous: the microporosity, as represented by $W_{0,N2}$, accounts
346 for more than 83% of the total pore volume for CS-CO_2 and more than 70% in the case
347 of CS-H_2O, which confirms the assumptions stated about the superior ability of carbon
348 dioxide to create microporosity during the carbon material activation. It has been
349 reported in the literature that carbon dioxide activation of almond shells and olive and
350 peach stones mainly results in the creation of microporosity, whilst steam activation
351 widens the microporosity from the early stages of the activation process, lowering the
352 micropore volume in the resulting activated carbons.[29,30] Likewise, according to the

353 shape of the N_2 adsorption isotherms (Fig. 2a), CS-CO_2 is nearly strictly microporous
354 and displays a pronounced elbow at low relative pressures whereas CS-H_2O shows a
355 linear increase in the N_2 uptake over the middle section of the isotherm and a
356 characteristic hysteresis loop that denotes the presence of mesoporosity. The presence of
357 mesoporosity could benefit the adsorption process dynamics as these pores could act as
358 feeding pores. Average micropore widths around 0.9 nm and characteristic energies
359 over 23 kJ mol^{-1} were obtained for both cherry stones-based ACs (Table 4).

360 Regarding the assessment of the narrow microporosity (of less than 1 nm in
361 size), the CO_2 adsorption isotherms of both ACs nearly overlapped up to relative
362 pressures of 0.02 and slightly diverged from there, where the adsorbed volume was
363 slightly higher for CS-CO_2 (Fig. 2b). Table 4 shows that similar features in terms of
364 narrow micropores are encountered in both ACs, although slightly higher values of
365 narrow micropore volume, $W_{0,CO2}$, and narrow micropore surface, $S_{mic,CO2}$, were
366 obtained for CS-CO_2. The characteristic energy also addresses a slight difference
367 between both ACs, pointing out a stronger interaction with CO_2 in the case of CS-H_2O.
368 The average narrow micropore width, $L_{0,CO2}$, for both adsorbents was between 0.7-
369 0.8 nm. The micropore size distributions in the narrow microporosity range (Fig. 2c)
370 reveal great similarities between both ACs. Nevertheless, the CO_2 activated carbon
371 shows a broader distribution in the 0.5-0.7 nm range and the steam activated carbon
372 presents a higher volume of micropores of approximately 0.5 nm.

373 It has been demonstrated that different porosity features (micro, meso and
374 macroporosity) are developed during the activation of biomass precursors according to
375 the activation conditions. This is in agreement with, previous works on biomass-derived
376 adsorbents.[4,5,7]

From the textural characterization of the cherry stones-based ACs it may be concluded that differences in the activation agent have an impact in the porosity development, although to a small extent, given that the preparation conditions were optimized in terms of a maximum CO_2 uptake at atmospheric pressure. The results showed that carbon dioxide activation promotes the development of microporosity whereas during steam activation micropores as well as mesopores are developed.

3.3 Adsorption and separation of CO_2/CH_4

The CO_2 uptakes obtained in the TGA at atmospheric pressure are higher than those of commercial activated carbons previously reported for CO_2 adsorption under similar conditions.[31] Moreover, they are in good agreement or are higher than the CO_2 uptakes of biomass-based carbon adsorbents evaluated for post-combustion capture.[27,28] Those results therefore show the potential of the produced activated carbons from cherry stones to be used as CO_2 adsorbents.

As a first step in the characterization of the two cherry stones-based ACs for CO_2/CH_4 separation purposes the pure component CO_2 and CH_4 adsorption isotherms were measured. Fig. 3a plots the experimental CO_2 and CH_4 adsorption isotherms at 30 ºC on both cherry stones-based ACs. The isotherms are Type I in IUPAC classification. Both CS activated carbons showed preferential adsorption of CO_2 over CH_4 in the pressure range tested. The microporosity in both samples seems large enough to neglect shape selectivity effects based on the kinetic diameters of the two gas molecules (3.30 Å for CO_2 and 3.80 Å for CH_4)[32]. However, the large quadrupolar moment of CO_2 (CH_4 does not hold a quadrupole moment) may account for such a difference in adsorption performance. The quadrupole moment produces a strong attraction to the adsorbent surface that results in an increased uptake. The polarizability

401 could also influence the adsorption performance. Nevertheless, both CO_2 and CH_4 show
402 high polarizability ($31x10^{-25}$ cm^3 for CO_2 and $26x10^{-25}$ cm^3 for CH_4)[32] and this
403 attraction force is much weaker than the quadrupole moment.

404 The performance of both materials to CO_2 and CH_4 adsorption presents great
405 similarities: the isotherms nearly overlapped at subatmospheric pressures but CS-CO_2
406 attains greater uptakes in the higher pressure range.

407 The fittings of the pure component CO_2 and CH_4 adsorption data at 30 ºC to the
408 Sips model (Eq. (6)) are also plotted (lines) in Fig. 3a. The optimal parameters and
409 squared relative errors from the performed fittings are listed in Table 5. Fig. 3a shows
410 that the Sips model fitted with good accuracy the experimental CO_2 and CH_4 adsorption
411 data over the tested pressure range. However, small deviations of the model from the
412 experimental CH_4 adsorption data occur in the pressure range above 5 bar. It has to be
413 borne in mind that during the optimization procedure, the saturation loading and the
414 parameter *n* (heterogeneity) for both adsorbates, CO_2 and CH_4, were considered equal.
415 This may impact to a greater extent the adsorbate with the weaker affinity, i.e., CH_4.
416 The goodness of the fitting is corroborated by the small values of the *SRE* reported in
417 Table 5. The affinity constants for CO_2 (b_{CO2}) are one order of magnitude greater than
418 those for CH_4 (b_{CH4}). The stronger affinity towards CO_2 is clearly reflected in the
419 greater experimental CO_2 uptakes from the adsorption isotherms and may account for
420 this difference. The values of the parameter *n* show certain heterogeneity in the system
421 that would not be adequately represented by the more conventional and theoretical
422 Langmuir equation.

423 Table 5 shows that the fitting of the adsorption data to the Sips model for both
424 cherry stones-based ACs delivers similar values of the optimized parameters.

425 Nevertheless, a small difference is seen in the value of the saturation loading, q_s, which
426 is higher in the case of the CS-CO_2 activated carbon. The fitted values of the saturation
427 loading, q_s, of both adsorbents are in good agreement with those found in the literature
428 for commercial activated carbons.[33]

429 Based on the fitted parameters from the pure component adsorption data, the
430 multicomponent Sips equation (Eq. (8)) was used to predict the adsorption performance
431 of CO_2 and CH_4 in binary mixtures at 30 ºC and 3 bar. These conditions were selected
432 to be representative of CO_2 separation from biogas streams. Fig. 3b shows the predicted
433 isotherms for both cherry stones-based activated carbons. The selectivity of both ACs to
434 separate CO_2 from CO_2/CH_4 binary mixtures was estimated from the following
435 expression:

436 $$S_{CO2/CH4} = \frac{q_{CO2}/q_{CH4}}{y_{CO2}/y_{CH4}} \quad (11)$$

437 where q_{CO2} and q_{CH4} where estimated from the multicomponent Sips model for the
438 different molar fractions of CO_2 (y_{CO2}) and CH_4 (y_{CH4}) in the binary mixtures.

439 The pure component CO_2 and CH_4 uptakes at 3 bar for both cherry stones-based
440 ACs are represented by the predicted multicomponent uptakes at CH_4 mole fractions of
441 0 and 1, respectively. As expected, both components show a decreasing trend in the
442 uptake with increasing mole fraction of the other component in the binary mixture. On
443 the other hand, the adsorption of CH_4 from a binary mixture seems to be more affected
444 than that of CO_2: CH_4 only holds a 27% of the pure component uptake when mixed with
445 CO_2 in a 50:50 binary mixture whereas CO_2 keeps a 65% of the pure component
446 adsorption capacity at 3 bar. On the other hand, the performance of both cherry stones-
447 based ACs is very similar in terms of the predicted CO_2 and CH_4 uptakes from binary
448 mixtures at 3 bar in agreement with the pure component experimental adsorption data at

449 this pressure. Moreover, both carbons show a decreasing trend in the selectivity to
450 separate CO_2 with increasing CH_4 mole fraction. At 3 bar the selectivity of the cherry
451 stones-based ACs for CO_2 remains in the range of 3.2-4, which is higher than the values
452 reported from experimental data of mesocarbon microbeads[34] and activated carbon
453 beads[35] as well as from molecular simulations in slit shaped pores.[36] On the other hand,
454 the values of the selectivity for both carbons differ and CS-H_2O shows enhanced
455 selectivity to separate CO_2 from CO_2/CH_4 binary mixtures at 3 bar than CS-CO_2. The
456 narrower character of the microporosity in CS-H_2O could account for such a difference.

457 **4 CONCLUSIONS**

458 Two low cost carbon adsorbents, CS-CO_2 and CS-H_2O, were produced from
459 cherry stones by single-step activation with CO_2 and steam, respectively. The effect of
460 activation temperature, heating rate and solid yield on the CO_2 uptake of the biomass-
461 based activated carbons was evaluated by means of the Response Surface Methodology.
462 The most influential variable on the CO_2 uptake was the activation temperature for the
463 CS-CO_2 adsorbent and the solid yield for the CS-H_2O activated carbon.

464 The highest CO_2 uptakes achieved at 25 ºC and atmospheric pressure were:
465 11.45 wt.% when the precursor was activated with carbon dioxide and 10.56% when the
466 precursor was activated with steam. Carbon dioxide activation promoted the
467 development of microporosity whereas during steam activation both micropores and
468 mesopores were developed. Pure and multicomponent adsorption tests at 3 bar on the
469 optimum activated carbons showed a similar CO_2/CH_4 separation performance for CS-
470 CO_2 and CS-H_2O. Even though the adsorbent activated with carbon dioxide showed a
471 slightly higher adsorption capacity, the activation with steam led to a slightly more
472 selective activated carbon to separate CO_2 from CH_4. In summary, due to their textural

development and low cost, the cherry stones-based activated carbons prepared are deemed as good adsorbents in CO_2 adsorption based applications; more precisely for the separation of CO_2 from CO_2/CH_4 mixtures.

Acknowledgements

This work was carried out with financial support from the Spanish MINECO (Project ENE2011-23467), co-financed by the European Regional Development Fund (ERDF) and from the Gobierno del Principado de Asturias (PCTI-GRUPIN14-079). N.A-G. acknowledges a FPI Predoctoral fellowship from the Spanish MINECO, co-financed by the European Social Fund.

References

1. Abatzoglou N, Boivin S. A review of biogas purification processes. *Biofuels Bioprod Biorefining* **3(1):**42-71 (2009).
2. Wang Q, Luo J, Zhong Z, Borgna A. CO_2 capture by solid adsorbents and their applications: current status and new trends. *Energy Environ Sci* **4(1):**42-55 (2011).
3. Rodríguez-Reinoso F, Molina-Sabio M. Activated carbons from lignocellulosic materials by chemical and/or physical activation: an overview. *Carbon* **30(7):**1111-1118 (1992).
4. Lua AC, Guo J. Activated carbon prepared from oil palm stone by one-step CO_2 activation for gaseous pollutant removal. *Carbon* **38(7):**1089-1097 (2000).
5. Yang K, Peng J, Xia H, Zhang L, Srinivasakannan C, Guo S. Textural characteristics of activated carbon by single step CO_2 activation from coconut shells. *J Taiwan Inst Chem Eng* **41(3):**367-372 (2010).
6. Savova D, Apak E, Ekinci E, Yardim F, Petrov N, Budinova T, et al. Biomass conversion to carbon adsorbents and gas. *Biomass Bioenerg* **21(2):**133-142 (2001).
7. Gergova K, Eser S. Effects of activation method on the pore structure of activated carbons from apricot stones. *Carbon* **34(7):**879-888 (1996).
8. Serna-Guerrero R, Belmabkhout Y, Sayari A. Influence of regeneration conditions on the cyclic performance of amine-grafted mesoporous silica for CO_2 capture: An experimental and statistical study. *Chem Eng Sci* **65(14):**4166-4172 (2010).
9. Mulgundmath V, Tezel FH. Optimisation of carbon dioxide recovery from flue gas in a TPSA system. *Adsorption* **16(6):**587-598 (2010).
10. Myers RH, Montgomery DC, *Response Surface Methodology: Process and Product Optimization Using Designed Experiments*, first ed. John Wiley & Sons Inc, New York (1995).
11. Nowicki P, Kazmierczak J, Pietrzak R. Comparison of physicochemical and sorption properties of activated carbons prepared by physical and chemical activation of cherry stones. *Powder Technol* **269(0):**312-319 (2015).

12. Olivares-Marín M, Del Prete V, Garcia-Moruno E, Fernández-González C, Macías-García A, Gómez-Serrano V. The development of an activated carbon from cherry stones and its use in the removal of ochratoxin A from red wine. *Food Control* **20(3):**298-303 (2009).
13. Jaramillo J, Gómez-Serrano V, Álvarez PM. Enhanced adsorption of metal ions onto functionalized granular activated carbons prepared from cherry stones. *J Hazard Mater* **161(2–3):**670-676 (2009).
14. Olivares-Marín M, Fernández-González C, Macías-García A, Gómez-Serrano V. Preparation of activated carbon from cherry stones by physical activation in air. Influence of the chemical carbonisation with H2SO4. *J Anal Appl Pyrolysis* **94(0):**131-137 (2012).
15. Gil MV, Martínez M, García S, Rubiera F, Pis JJ, Pevida C. Response surface methodology as an efficient tool for optimizing carbon adsorbents for CO_2 capture. *Fuel Process Technol* **106(0):**55-61 (2013).
16. Baş D, Boyacı İH. Modeling and optimization I: Usability of response surface methodology. *J Food Eng* **78(3):**836-845 (2007).
17. Lozano-Castelló D, Cazorla-Amorós D, Linares-Solano A. Usefulness of CO_2 adsorption at 273 K for the characterization of porous carbons. *Carbon* **42(7):**1233-1242 (2004).
18. Brunauer S, Emmett PH, Teller E. Adsorption of Gases in Multimolecular Layers. *J Am Chem Soc* **60(2):**309-319 (1938).
19. Dubinin MM, Porous structure and adsorption properties of active carbons, in: Walker PL, editor. *Chem Phys Carbon*. Marcel Dekker Inc., New York, pp. 51-119 (1966).
20. Stoeckli F, Ballerini L. Evolution of microporosity during activation of carbon. *Fuel* **70(4):**557-559 (1991).
21. Stoeckli F, Characterization of microporous carbons by adsorption and immersion techniques, in: Patrick JW, editor. *Porosity in carbons-characterization and applications*. Arnold, London, pp. 67-92 (1995).
22. Vishnyakov A, Ravikovitch PI, Neimark AV. Molecular Level Models for CO_2 Sorption in Nanopores. *Langmuir* **15(25):**8736-8742 (1999).
23. Martín CF, García S, Beneroso D, Pis JJ, Rubiera F, Pevida C. Precombustion CO_2 capture by means of phenol–formaldehyde resin-derived carbons: From equilibrium to dynamic conditions. *Sep Purif Technol* **98(0):**531-538 (2012).
24. García S, Pis JJ, Rubiera F, Pevida C. Predicting Mixed-Gas Adsorption Equilibria on Activated Carbon for Precombustion CO_2 Capture. *Langmuir* **29(20):**6042-6052 (2013).
25. Rudziński W, Nieszporek K, Moon H, Rhee H-K. On the theoretical origin and applicability of the potential theory approach to predict mixed-gas adsorption on solid surfaces from single-gas adsorption isotherms. *Chem Eng Sci* **50(16):**2641-2660 (1995).
26. Martín CF, Plaza MG, Pis JJ, Rubiera F, Pevida C, Centeno TA. On the limits of CO_2 capture capacity of carbons. *Sep Purif Technol* **74(2):**225-229 (2010).
27. González AS, Plaza MG, Rubiera F, Pevida C. Sustainable biomass-based carbon adsorbents for post-combustion CO_2 capture. *Chem Eng J* **230(0):**456-465 (2013).
28. Plaza MG, González AS, Pis JJ, Rubiera F, Pevida C. Production of microporous biochars by single-step oxidation: Effect of activation conditions on CO_2 capture. *Appl Energy* **114(0):**551-562 (2014).

29. Rodríguez-Reinoso F, Molina-Sabio M, González MT. The use of steam and CO_2 as activating agents in the preparation of activated carbons. *Carbon* **33(1):**15-23 (1995).
30. Molina-Sabio M, Gonzalez MT, Rodriguez-Reinoso F, Sepúlveda-Escribano A. Effect of steam and carbon dioxide activation in the micropore size distribution of activated carbon. *Carbon* **34(4):**505-509 (1996).
31. Pevida C, Plaza MG, Arias B, Fermoso J, Rubiera F, Pis JJ. Surface modification of activated carbons for CO_2 capture. *Appl Surf Sci* **254(22):**7165-7172 (2008).
32. Bárcia PS, Bastin L, Hurtado EJ, Silva JAC, Rodrigues AE, Chen B. Single and Multicomponent Sorption of CO_2, CH_4 and N_2 in a Microporous Metal-Organic Framework. *Sep Sci Technol* **43(13):**3494-3521 (2008).
33. Ahmadpour A, Wang K, Do DD. Comparison of models on the prediction of binary equilibrium data of activated carbons. *AlChE J* **44(3):**740-752 (1998).
34. Peng X, Wang W, Xue R, Shen Z. Adsorption separation of CH_4/CO_2 on mesocarbon microbeads: Experiment and modeling. *AlChE J* **52(3):**994-1003 (2006).
35. Shao X, Feng Z, Xue R, Ma C, Wang W, Peng X, et al. Adsorption of CO_2, CH_4, CO_2/N_2 and CO_2/CH_4 in novel activated carbon beads: Preparation, measurements and simulation. *AlChE J* **57(11):**3042-3051 (2011).
36. Kurniawan Y, Bhatia SK, Rudolph V. Simulation of binary mixture adsorption of methane and CO_2 at supercritical conditions in carbons. *AlChE J* **52(3):**957-967 (2006).

582 **Figure captions**

583 Fig. 1. Response surface and contour plots for the CO_2 capture capacity as a function of
584 the activation temperature and solid yield corresponding to the carbon dioxide
585 activated-CS (a) and steam activated-CS (b) adsorbents.

586 Fig. 2. N_2 adsorption isotherms at -196 ºC (a), CO_2 adsorption isotherms at 0 ºC (b) and
587 micropore size distributions assessed from the NLDFT-CO_2 slit shaped carbon model
588 (c) for the optimum cherry stones-based activated carbons.

589 Fig. 3. CO_2 and CH_4 adsorption isotherms at 30 ºC (a) and predicted CO_2 and CH_4
590 adsorption and selectivity for binary CO_2/CH_4 mixtures at 3 bar and 30 ºC (b) for the
591 cherry stones-based activated carbons.

592

593 **Table 1** Proximate and ultimate analyses of the raw cherry stones (CS) used as carbon precursor in the present work

Sample	CS
Proximate analysis[a]	
Moisture (wt.%)	3.90
Volatile matter (wt.%, db)	82.78
Ash (wt.%, db)	0.40
Fixed carbon (wt.%, db)[b]	16.82
Ultimate analysis (wt.%, daf)[a]	
C	52.76
H	6.18
N	0.76
S	0.02
O[b]	40.28

594 db: dry basis; daf: dry and ash free bases.
595 [a] The proximate analysis was conducted in a LECO TGA-601, and the ultimate analysis in a LECO CHNS-932.
596 [b] Calculated by difference.
597

598

599

Table 2 Independent variables and experimental values of the response variable for the central composite design (CCD) using the CS adsorbents

Run	Independent variables			Response
	T (ºC)	*HR* (ºC min^{-1})	*Y* (%)	CO_2 capture (%)
Carbon dioxide activated-CS				
1	790.5 (-1)	12.03 (-1)	9.03 (-1)	10.57
2	909.5 (+1)	12.03 (-1)	9.03 (-1)	11.52
3	790.5 (-1)	17.97 (+1)	9.03 (-1)	10.61
4	909.5 (+1)	17.97 (+1)	9.03 (-1)	10.97
5	790.5 (-1)	12.03 (-1)	14.97 (+1)	10.54
6	909.5 (+1)	12.03 (-1)	14.97 (+1)	10.95
7	790.5 (-1)	17.97 (+1)	14.97 (+1)	10.44
8	909.5 (+1)	17.97 (+1)	14.97 (+1)	10.97
9[a]	850.0 (0)	15.00 (0)	12.00 (0)	11.24
10	750.0 (-1.682)	15.00 (0)	12.00 (0)	9.60
11	950.0 (+1.682)	15.00 (0)	12.00 (0)	11.22
12	850.0 (0)	10.00 (-1.682)	12.00 (0)	11.89
13	850.0 (0)	20.00 (+1.682)	12.00 (0)	11.35
14	850.0 (0)	15.00 (0)	7.00 (-1.682)	10.03
15	850.0 (0)	15.00 (0)	17.00 (+1.682)	10.99
Steam activated-CS				
1	790.5 (-1)	12.03 (-1)	10.04 (-1)	9.64
2	909.5 (+1)	12.03 (-1)	10.04 (-1)	9.72
3	790.5 (-1)	17.97 (+1)	10.04 (-1)	9.56
4	909.5 (+1)	17.97 (+1)	10.04 (-1)	9.58
5	790.5 (-1)	12.03 (-1)	18.96 (+1)	10.10
6	909.5 (+1)	12.03 (-1)	18.96 (+1)	10.15
7	790.5 (-1)	17.97 (+1)	18.96 (+1)	9.83
8	909.5 (+1)	17.97 (+1)	18.96 (+1)	10.54
9[a]	850.0 (0)	15.00 (0)	14.50 (0)	10.50
10	750.0 (-1.682)	15.00 (0)	14.50 (0)	9.95
11	950.0 (+1.682)	15.00 (0)	14.50 (0)	10.13
12	850.0 (0)	10.00 (-1.682)	14.50 (0)	10.44
13	850.0 (0)	20.00 (+1.682)	14.50 (0)	10.66
14	850.0 (0)	15.00 (0)	7.00 (-1.682)	8.42
15	850.0 (0)	15.00 (0)	22.00 (+1.682)	8.90

[a] Central point mean of six replicates

T: activation temperature; *HR*: heating rate; *Y*: solid yield.

607
608 **Table 3** Results of multiple regression analysis and ANOVA for the fit of the polynomial model to the CO_2 capture capacity
609 experimental data of activated carbons

	Carbon dioxide activated-CS				Steam activated-CS			
	Coded coefficient	Sum of squares	DF	*p*-value	Coded coefficient	Sum of squares	DF	*p*-value
Intersection	11.235	758.836	1	0.000	10.494	662.037	1	0.000
T	0.364	1.812	1	0.002	0.085	0.099	1	0.125
HR	-0.110	0.164	1	0.229	0.020	0.627	1	0.704
Y	0.062	0.052	1	0.485	0.214	0.005	1	0.002
T^2	-0.292	1.229	1	0.006	-0.124	0.220	1	0.033
HR^2	0.136	0.265	1	0.135	0.057	5.387	1	0.276
Y^2	-0.257	0.950	1	0.013	-0.611	0.046	1	0.000
T·HR	-0.059	0.028	1	0.609	0.075	0.054	1	0.283
T·Y	-0.046	0.017	1	0.687	0.083	0.045	1	0.241
HR·Y	0.054	0.023	1	0.640	0.043	0.014	1	0.534
T·HR·Y	0.089	0.063	1	0.445	0.090	0.065	1	0.204
Model		4.647	10	0.014		6.578	10	0.000
Residual		0.887	9			0.311	9	
Total		5.535	19			6.889	19	
Lack-of-fit		0.641	4	0.114		0.189	4	0.243
Pure error		0.247	5			0.122	5	
R^2	0.840				0.955			
Adj-R^2	0.662				0.905			
AAD (%)	2.07				1.31			

610

611

612

613 **Table 4** Textural characteristics of the optimum cherry stones-based activated carbons

Sample	N_2 adsorption at -196 ºC						CO_2 adsorption at 0 ºC			
	S_{BET} ($m^2\ g^{-1}$)	V_p ($cm^3\ g^{-1}$)	$W_{0,N2}$ ($cm^3\ g^{-1}$)	$L_{0,N2}$ (nm)	$E_{0,N2}$ (kJ mol^{-1})	$S_{mic,N2}$ ($m^2\ g^{-1}$)	$W_{0,CO2}$ ($cm^3\ g^{-1}$)	$L_{0,CO2}$ (nm)	$E_{0,CO2}$ (kJ mol^{-1})	$S_{mic,CO2}$ ($m^2\ g^{-1}$)
CS-CO_2	1045	0.48	0.40	0.93	23.0	848	0.35	0.78	25.3	906
CS-H_2O	998	0.53	0.38	0.89	23.6	847	0.33	0.74	26.0	899

614

615

616

617 **Table 5** Optimal parameters calculated from the fitting of the pure component CO_2 and CH_4 adsorption isotherms at 30 ºC to the
618 Sips model

Sample	q_s (mmol g^{-1})	n	b_{CO2}	b_{CH4}	*SRE (%)*
CS-CO_2	10.45	1.40	$1.7x10^{-3}$	$4.7x10^{-4}$	3.27
CS-H_2O	9.31	1.39	$2.1x10^{-3}$	$5.2x10^{-4}$	2.42

619

620

621

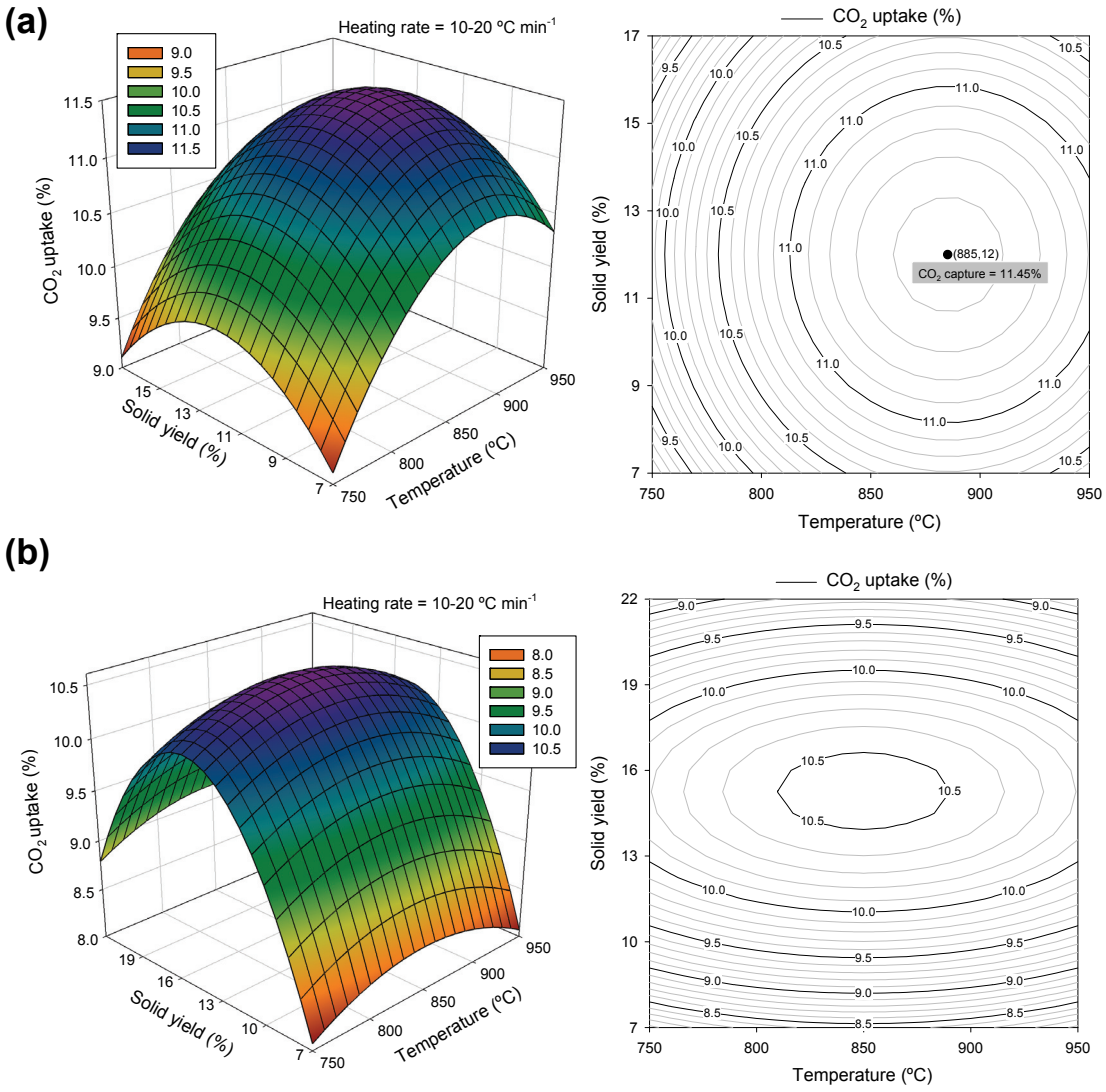

622

623 **Fig. 1** Response surface and contour plots for the CO_2 capture capacity as a function of

624 the activation temperature and solid yield corresponding to the carbon dioxide

625 activated-CS (a) and steam activated-CS (b) adsorbents.

626

627

628

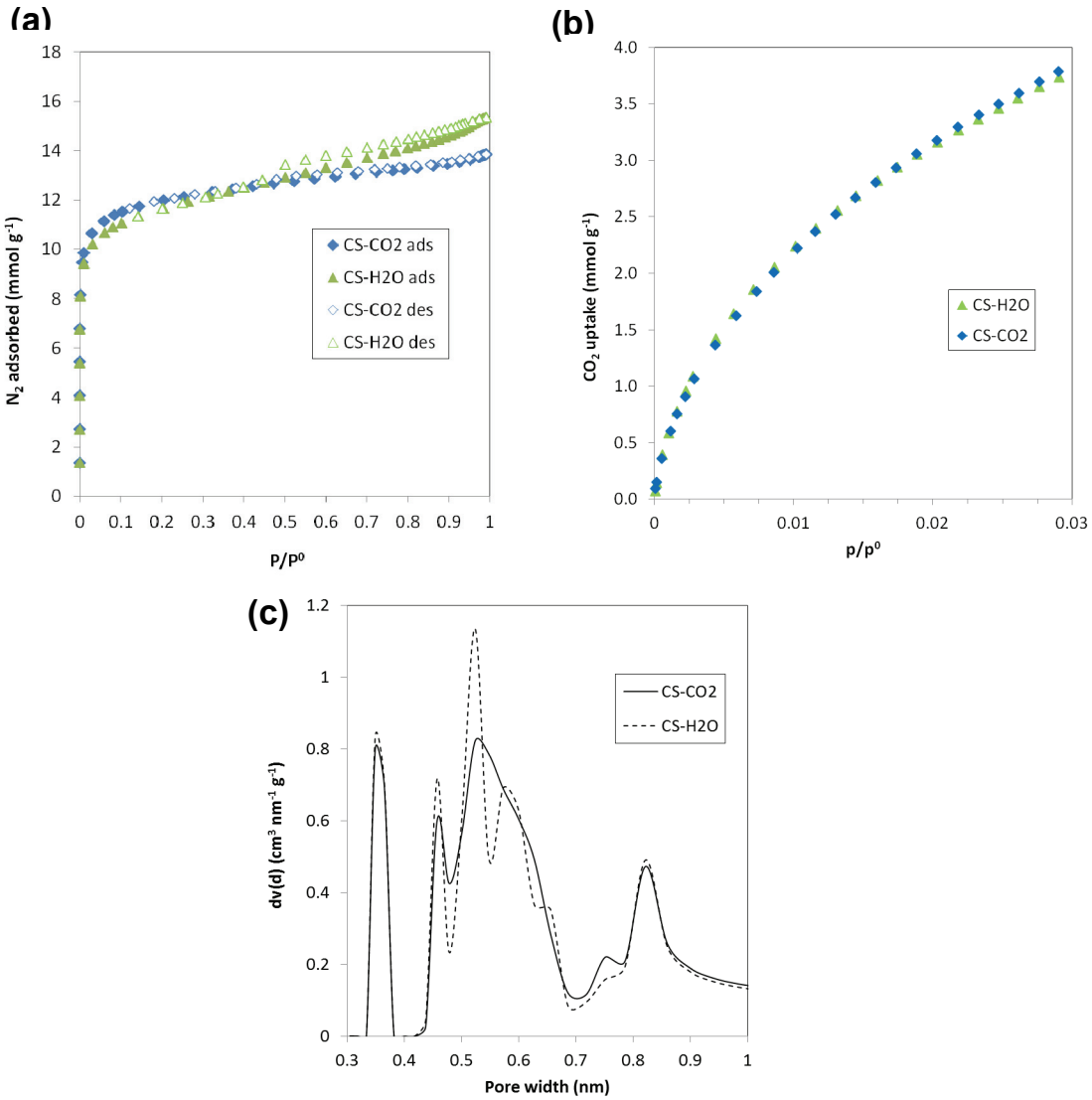

629

630 **Fig. 2** N_2 adsorption isotherms at -196 ºC (a), CO_2 adsorption isotherms at 0 ºC (b) and

631 micropore size distributions assessed from the NLDFT-CO_2 slit-shaped carbon model

632 (c) of the optimum cherry stones-based activated carbons.

633

634

635

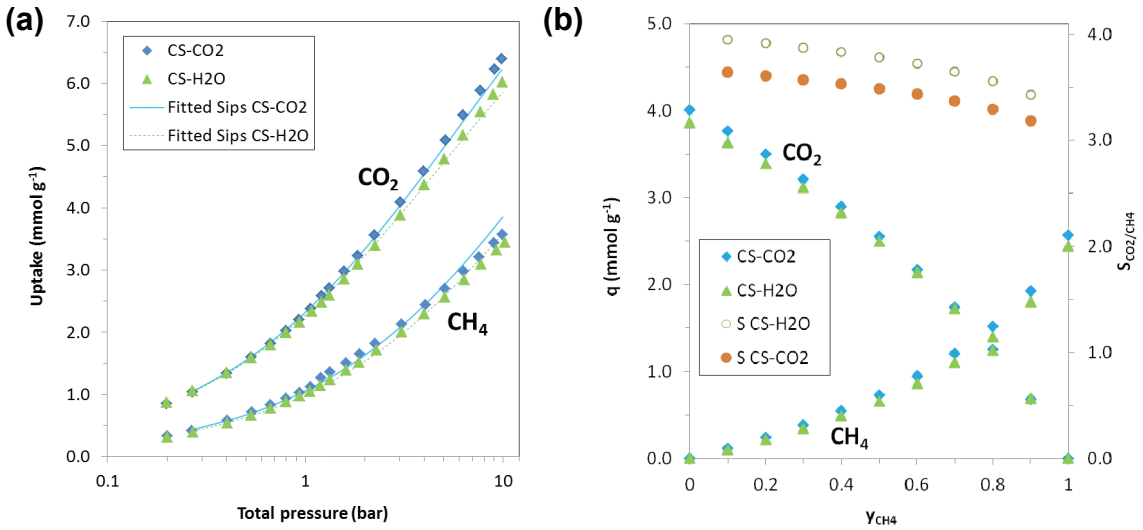

636

637 **Fig. 3** CO_2 and CH_4 adsorption isotherms at 30 ºC (a) and predicted CO_2 and CH_4

638 adsorption and selectivity for binary CO_2/CH_4 mixtures at 3 bar and 30 ºC (b) for the

639 cherry stones-based activated carbons.

640

641

642